JOURNAL OF MATERIALS SCIENCE 27 (1992) 2580–2588

Ultrafine aluminium nitride powder produced by plasma-assisted chemical vapour deposition of trimethylaluminium

KWANG-HO KIM*, CHIN-HSIUNG HO, H. DOERR, C. DESHPANDEY, R. F. BUNSHAH
Department of Materials Science and Engineering, University of California, Los Angeles, CA 90024, USA

Plasma-assisted chemical vapour deposition of trimethylaluminium (TMAl) with ammonia (NH_3) as reactive gas, was used to prepare aluminium nitride (AlN) ultrafine powder. The effect of r.f. current, susceptor temperature and TMAl concentration on particle formation was studied. High r.f. current activated the gas-phase reaction sufficiently to obtain considerable powder formation. It was observed that increasing susceptor temperature led to an increase of powder formation rate and improved the crystallinity of as-synthesized AlN powder as well. Increasing TMAl concentration, on the other hand, led to an increase of powder formation rate of AlN, while much higher TMAl concentration induced the formation of an aluminium carbide (Al_4C_3) phase due to dissociation of the methyl radicals instead of the Al–C bond.

1. Introduction and objective

Extremely small particles of less than 0.1 μm size are termed ultrafine particles, and have been investigated [1, 2] during the last few decades. Ultrafine nitride particles [3, 4] possess promising optical and mechanical properties different from those of the corresponding bulk materials. They are therefore attractive for applications such as low-temperature sintering, catalysis, plasma gun coatings, electronic devices, gas sensors, etc. Nevertheless, there have been relatively few investigations [5–7] of the synthesis of nitride fine particles, and their main preparation method has been reactive evaporation [8, 9].

Chemical vapour deposition (CVD) [10, 11] is one of the most widely used techniques for preparation of ultrafine powder of a large variety of elements and compounds with controlled composition, structure, and purity. However, the conventional CVD process suffers from limitations due to the requirement of high reaction temperature for the dissociation of source gases. The reaction temperature in the CVD process can be significantly reduced when organometallic compounds are used as source materials. Reaction temperatures can be reduced further if plasma activation is employed to enhance the chemical reactions forming the compounds.

In view of the above, synthesis of ultrafine AlN powder by plasma-assisted chemical vapour deposition (PACVD) technique using trimethylaluminium (TMAl) and ammonia (NH_3) as reaction gases has been explored. The effect of experimental parameters such as r.f. current, temperature, and composition of reactant gas mixture on formation rate, structure, and composition of the ultrafine powders has been investigated.

2. Experimental procedure

AlN ultrafine particles were synthesized by the PACVD method using TMAl, $Al(CH_3)_3$, and NH_3 as reactants. A schematic diagram of the deposition system used for our powder synthesis is shown in Fig. 1. It consists of a horizontally mounted 7.5 cm diameter, 62 cm long quartz tube with associated pumping and gas feed system. A susceptor (S1) is located at the centre of a quartz tube and heated by using 60 kHz r.f. source. The variation of susceptor temperature depends on the r.f. current. Synthesized particles were collected on the walls of the quartz tube as well as on TEM grids (S2) located about 15 cm downstream from the hot susceptor. Silicon substrates (only for powder-collecting purposes) were placed on to the hot susceptor to deposit a film simultaneously with powder synthesis.

Nitrogen (99.999% purity) was used as a carrier gas for introducing TMAl into the reaction chamber. The concentration of TMAl in the reaction chamber was controlled by the flow rate of nitrogen through the TMAl bubbler kept at room temperature and a pressure of 1 atm. The nitrogen flow rate was measured using a calibrated rotometer. Ammonia gas was also introduced in the reaction chamber via a calibrated rotometer. The ratio of TMAl:NH_3 in the reaction chamber was varied by adjusting the flow rate of

* On leave from: Department Inorganic Materials Engineering, Pusan National University, Pusan 609-735, Korea.

0022–2461

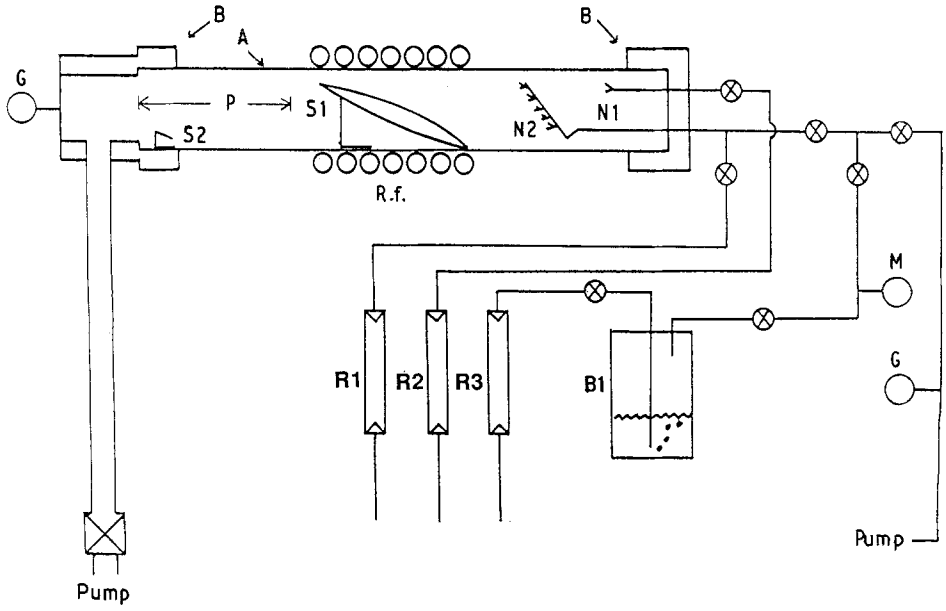

Figure 1 Schematic diagram of the experimental apparatus. A, Quartz tube; B, brass holder; R1, R2, R3, rotometer; M, mechanical gauge; G, convectron gauge (thermocouple gauge); N1, nozzle for NH_3; N2, nozzle for TMA and carrier N_2; P, particle collection region; S1, hot susceptor; S2, holder for TEM grid.

nitrogen and ammonia. The total reaction pressure was measured by a convectron gauge (thermocouple gauge) calibrated for nitrogen. The total reaction pressure in all the experiments was kept constant at 10 torr (1 torr = 1.3332×10^2 Pa) by using a throttle valve located above the mechanical pump.

To investigate the effect of the plasma intensity on powder formation at a constant reaction temperature, experiments were carried out using three different susceptors made of graphite, copper, and stainless steel. The rationale for this approach is as follows.

For a given r.f. current, the temperature of a susceptor is a function of the susceptor material. Hence to obtain the same temperature with different susceptor materials, one has to use different r.f. currents through the coupling coil as shown in Fig. 2 for copper, stainless steel, and graphite susceptors, respectively. The plasma conditions are primarily dependent on r.f. current. Thus by carrying out experiments using the three different susceptors, e.g. copper, stainless steel, and graphite, at a fixed temperature, the effect of the plasma intensity at a given temperature can be estimated. Similarly by keeping the r.f. current, i.e. the plasma condition, constant but using different susceptors, the effect of temperature on particle formation at a constant plasma condition can be estimated. The above procedures were followed in this study to investigate the effect of plasma conditions on powder formation.

The typical experimental procedures were as follows. The background pressure of the reaction chamber was first evacuated to below 20 mtorr, and ammonia gas was then introduced. In an ammonia gas pressure of around 10 torr, the susceptor (S1) was heated by increasing the r.f. current to a desired value. On reaching a stabilized susceptor temperature, TMAl vapour carried by nitrogen gas was introduced into the chamber. The reactants passed the elliptically shaped susceptor (S1), around which a heated zone

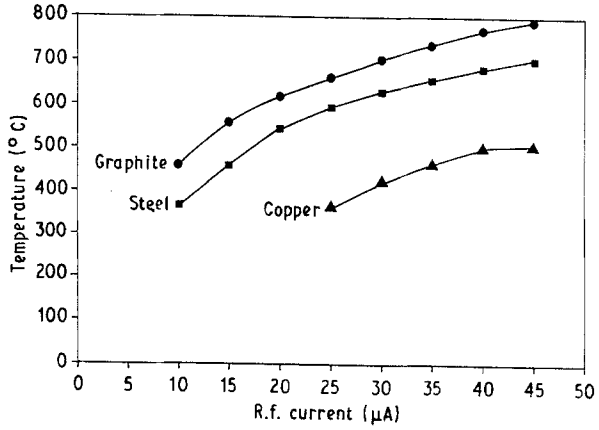

Figure 2 Temperature versus r.f. current (graphite, stainless steel, and copper susceptor).

was obtained, and reacted to form AlN particles. These ultra-fine particles were collected downstream on the carbon-coated TEM grids and on the cold wall of the quartz tube.

The structure of the collected particles was analysed by X-ray diffraction using nickel filtered CuK_α radiation. Particle size was estimated from the transmission electron micrographs. Production rate of particles was measured by weighing powders collected on a specific area of the quartz tube as shown in Fig. 1.

3. Results

Fig. 3 shows the effect of r.f. current on powder formation rate at a fixed temperature of 500 °C. For a r.f. current of 12 and 17 μA, no powder formation was observed, but a thin film was formed on the wall of the reactor tube in the cold region as well as on the TEM grid (S2) located downstream from the hot susceptor zone. The film consisted of an amorphous phase and exhibited a smooth surface morphology as observed

by electron diffraction and TEM, respectively. At a higher r.f. current of 40 μA, a detectable amount of powder was formed and collected on the cold wall. A typical X-ray diffraction pattern of the powder formed under these conditions is given in Fig. 5a, below, indicating that the crystalline AlN powder is formed at the higher r.f. current. It can, therefore, be inferred that the enhanced plasma activation at higher r.f. currents leads to formation of crystalline particles even at substrate temperatures as low as 500 °C.

The effect of temperature on powder formation at a fixed r.f. current of 40 μA is shown in Fig. 4. It can be seen that the powder formation rate increases with increase of susceptor temperature. The corresponding X-ray diffraction patterns of the powder prepared at different temperatures are shown in Fig. 5. It is observed that the intensity and sharpness of the diffraction peaks increase with increasing susceptor temperature. Moreover, the calculated *d*-values show good agreement with AlN standard [12] indicating that the formation of crystalline single-phase AlN is enhanced with increasing susceptor temperature.

Transmission electron micrographs of AlN ultrafine powder prepared at various temperatures are shown in Fig. 6a–c, showing that agglomerated particles were formed within the temperature range explored in this study. Particle agglomeration made it difficult to estimate the effect of temperature on individual particle size. Electron diffraction patterns (EDP) of the powder prepared at high temperature (770 °C) indicate that small-grain crystalline particles are formed. The calculated *d*-value ratios from the EDP show excellent agreement with standard X-ray *d*-values, thus confirming the AlN structure of the particles.

The effect of TMAl concentration on powder formation at a fixed r.f. current of 40 μA and susceptor temperature of 770 °C is shown in Fig. 7. It is observed that powder formation rate increased as $TMAl/NH_3$ ratio increased from 4.5×10^{-4} to 9.6×10^{-3}. An increase of TMAl concentration enhanced particle agglomeration as seen from the transmission electron micrographs of AlN particles prepared under various conditions shown in Fig. 8. X-ray diffraction patterns indicated that particles produced under the above conditions were predominantly single-phase AlN. However when the $TMAl/NH_3$ ratio was further increased, another phase appeared along with the AlN phase. X-ray diffraction pattern of powders prepared at a condition of high $TMAl/NH_3$ ratio beyond the above range is shown in Fig. 9a. The small peak at 55° (2θ) in Fig. 9a does not belong to the AlN phase, thus indicating that powder prepared at this condition is a mixture of an AlN phase and a different phase which was simultaneously produced during the gas-phase reaction. To reveal the phase corresponding to the 55° peak of Fig. 9a, powder was prepared at much higher TMAl concentration, which was obtained by reducing the bubbling pressure of nitrogen through TMAl to around 1333 Pa (10 torr). The X-ray diffraction pattern of powder (Fig. 9b) prepared under this condition corresponds to Al_4C_3.

Transmission electron micrographs of the mixed-phase AlN/Al_4C_3 powder and of Al_4C_3 powder are shown respectively in Fig. 10a and b. For reference, Fig. 11 shows the X-ray diffraction patterns of AlN thin film and Al_4C_3 thin film coated on (1 1 1)-type silicon (Si) wafer substrates placed on to the hot susceptor. The X-ray diffraction pattern of Fig. 11a corresponds to AlN and was obtained under the same reaction conditions as Fig. 5c. The X-ray diffraction pattern of Fig. 11b corresponds to Al_4C_3 and was obtained under the same reaction conditions as Fig. 9b.

4. Discussion

Particle formation and growth are related to two basic phenomena. The first step is the formation of homogeneous nuclei by the gas-phase reaction. After nucleation, particles can grow by two possible processes. One is vapour deposition on the particle surface, and the other is growth by collision and coalescence of

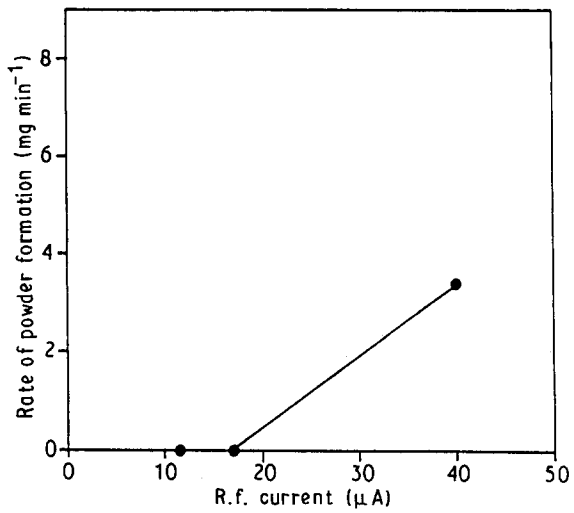

Figure 3 Rate of powder formation with variation of r.f. current (susceptor temperature 500 °C, $TMAl/NH_3$, 4.8×10^{-3}, NH_3 170 sccm, reactor pressure 10 torr).

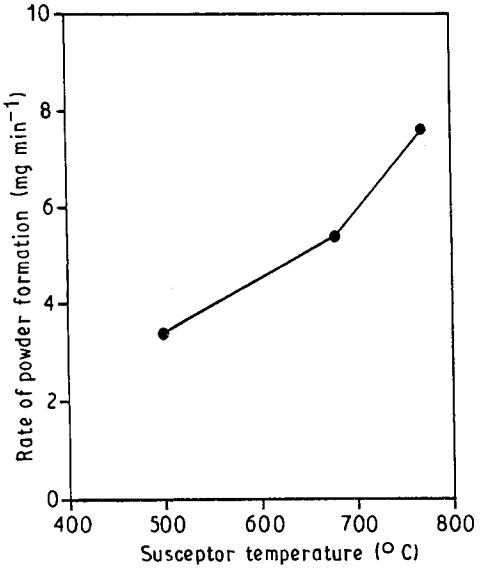

Figure 4 Rate of powder formation and particle size with variation of susceptor temperature. (r.f. current 40 μA, $TMAl/NH_3$ 4.8×10^{-3}, NH_3 170 sccm, reactor pressure; 1333 Pa/10 torr).

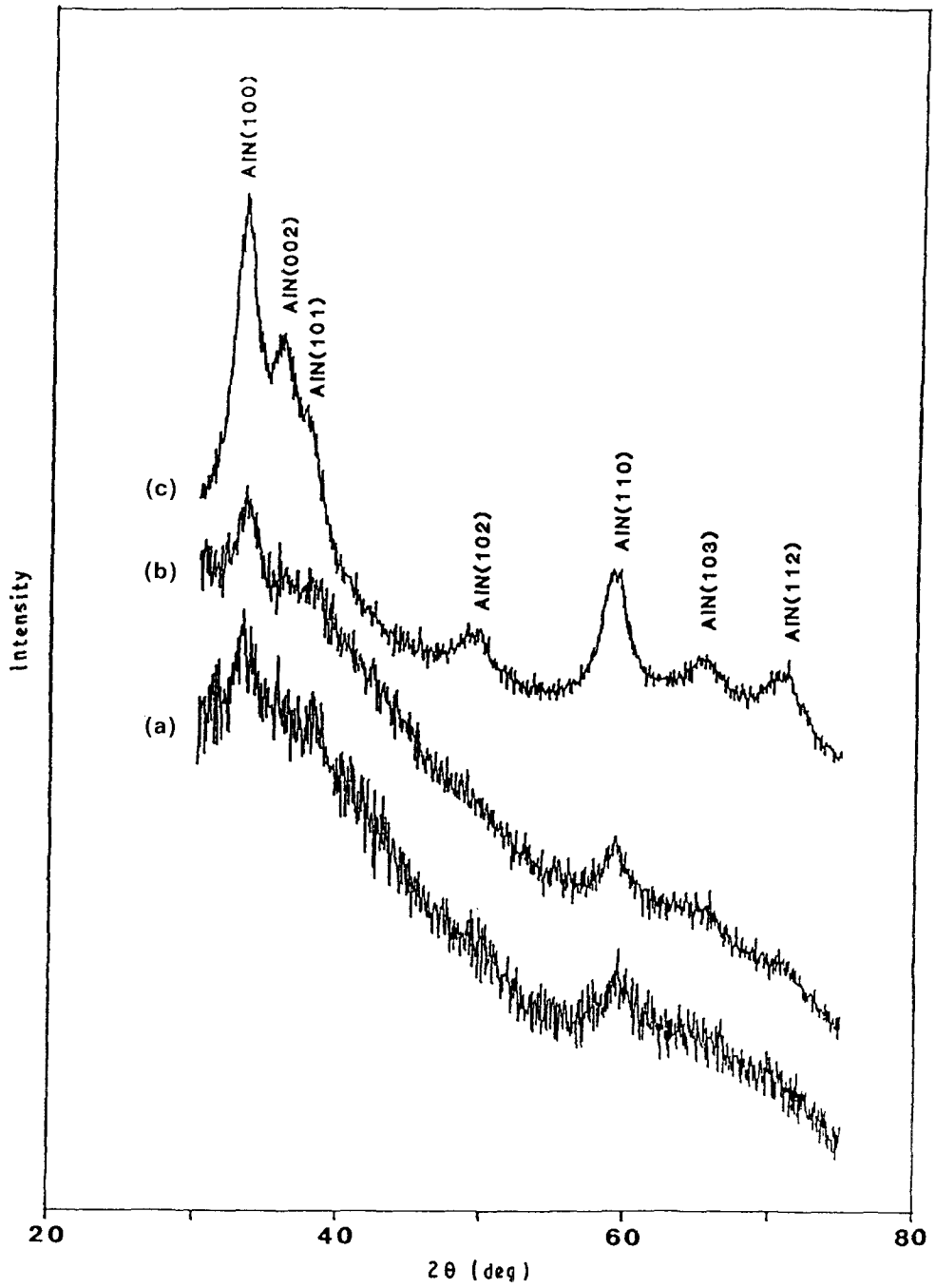

Figure 5 X-ray diffraction patterns with variation of susceptor temperature: (a) 500 °C, (b) 680 °C, (c) 770 °C. (Reaction conditions same as Fig. 4.)

particles (nuclei). Using classical nucleation theory, the critical radius of a stable nucleus is given from simple classical thermodynamics [13]

$$r_{crit} = 2\gamma[\rho RT \ln S]^{-1} \quad (1)$$

where ρ is the density, R the gas constant, T the temperature, γ the specific surface energy, and S the supersaturation ratio, i.e. true vapour pressure divided by equilibrium vapour pressure at the actual temperature.

In many chemical reaction systems for the synthesis of oxides, carbides and nitrides, the equilibrium vapour pressure over those phases is extremely low. Thus, even a low reactant gas pressure results in high thermodynamic supersaturation. The critical radius to form a stable nucleus calculated from Equation 1 is generally close to a few atomic diameters. It is therefore inferred that once the monomer of those phases is formed by chemical reaction, the monomer becomes a stable nucleus and grows into bigger particles according to the growth mechanism given below.

In the growth of particles after nucleation, if the chemical reaction in the gas phase is assumed to be instantaneous, growth can be predicted by Brownian collision and coalescence theory. If the reaction is not instantaneous, vapour deposition on particle surfaces can occur in conjunction with collision and coalescence.

In our system using TMAl and NH_3 gas, the overall reaction for AlN formation may be expressed [14] as

$$(CH_3)_3Al + NH_3 \rightarrow AlN + 3CH_4 \quad (2)$$

The reaction rate at low temperature is not high, even though the reactant gas phase is highly saturated

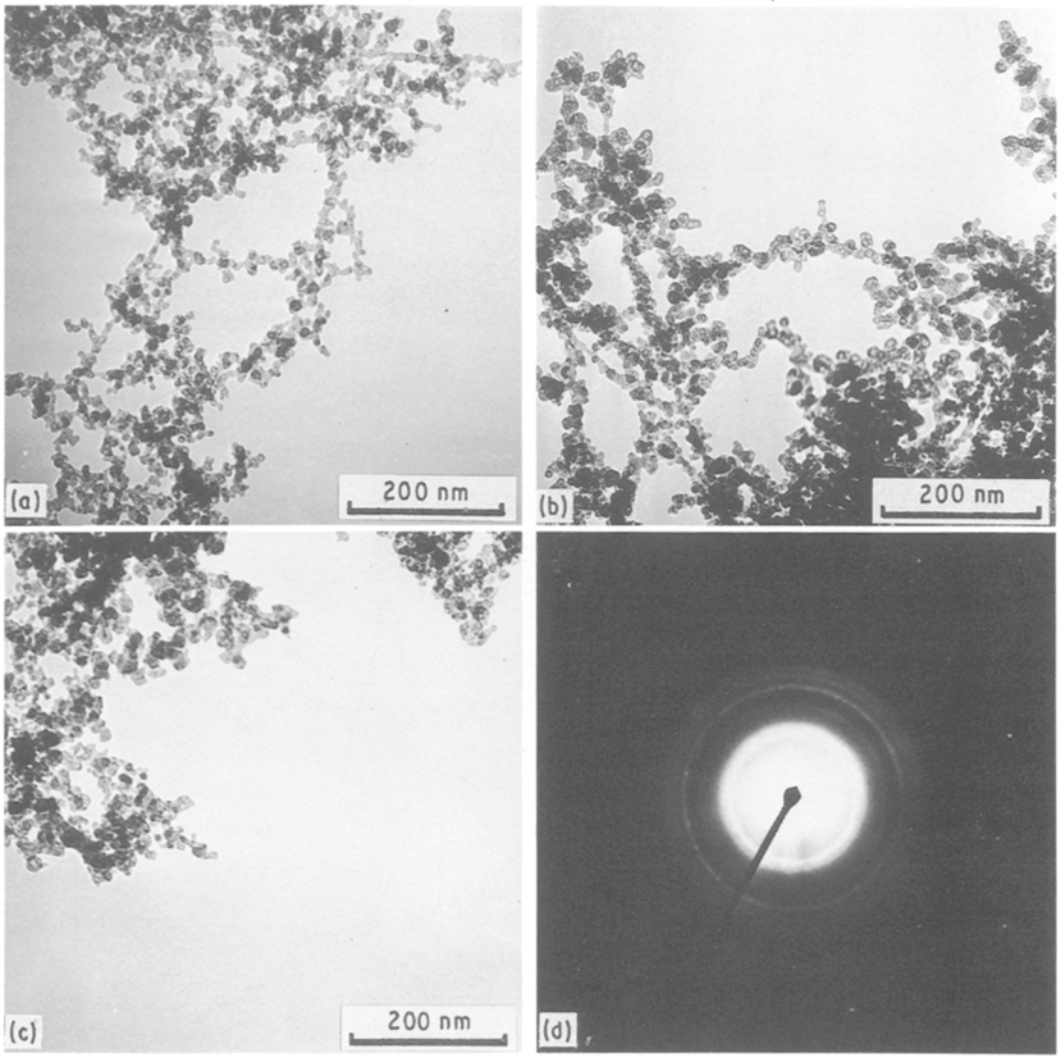

Figure 6 Transmission electron micrographs of AlN particles with variation of susceptor temperature. (a) 500 °C, (b) 680 °C, (c) 770 °C, (d) diffraction pattern of (c). (Reaction conditions same as Fig. 5.)

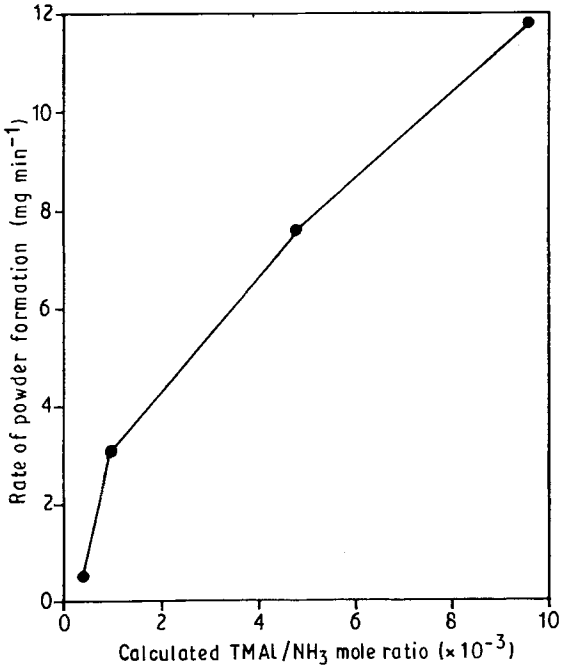

Figure 7 Rate of AlN powder formation with variation of input TMAl/NH_3 ratio. (r.f. current 40 μA, susceptor temperature, 770 °C, NH_3 170 sccm, reactor pressure 1333 Pa/10 torr.)

thermodynamically. Thus, the rate of the chemical reaction of Equation 2 is considered to be the rate controlling step in the synthesis of AlN particles in our system. Hence, particle growth occurs both by collision and coalescence, as well as by vapour deposition on to particle surfaces.

This chemical reaction can be activated by either thermal energy or plasma energy. Let us now consider the effects of various parameters.

4.1. R.f. current effect

In the r.f.-excited reactor, radicals are created from precursor gases, i.e. TMAl and NH_3 in the plasma volume. Although the processes occurring in the plasma volume cannot be quantified, the decomposition rate, R_i, to the first approximation, can be represented as [15]

$$R_i = N_e K_i P \quad (3)$$

where N_e is the electron density, K_i is the rate constant for the reaction, and P is the concentration of the reactant. The rate constant is related to both the gas temperature resulting from thermal energy, and the

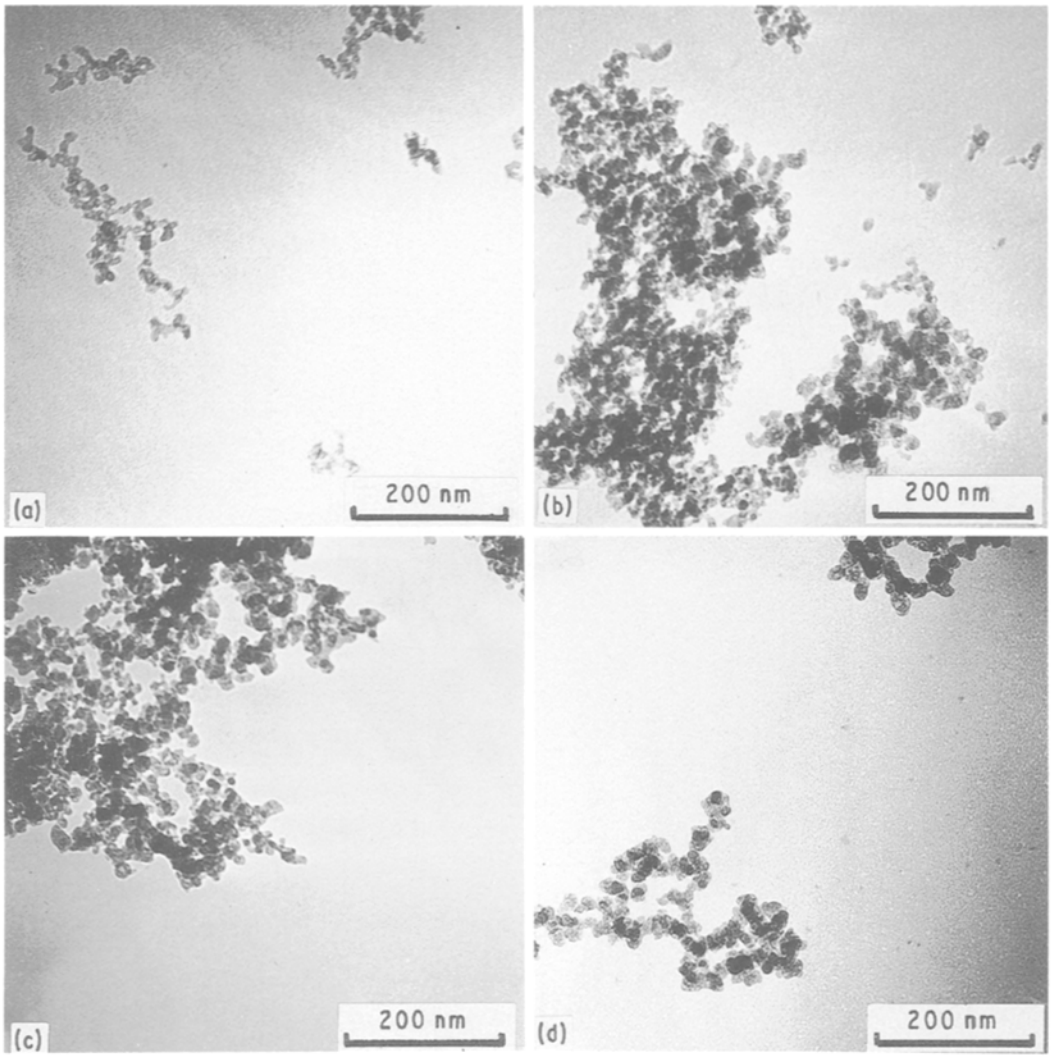

Figure 8 Transmission electron micrographs of AlN particles with variation of input $TMAl/NH_3$ ratio. (Reaction conditions same as Fig. 7.) $TMAl/NH_3$ ratios: (a) 4.5×10^{-4}, (b) 9.6×10^{-4}, (c) 4.8×10^{-3} and (d) 9.6×10^{-3}.

electron temperature, which is dependent on gas pressure and r.f. power. At constant temperature and pressure, K_i is constant and the r.f. current is primarily related to the electron concentration, N_e. Thus, a higher r.f. current results in higher electron density and subsequently increased monomer decomposition rate, R_i.

The results shown in Fig. 3 were obtained under conditions of highly supersaturated reactant gases. A high r.f. current of 40 μA with high supersaturation of reactant gases was sufficient to cause homogeneous nucleation of the particles in the gas phase.

4.2. Temperature effect

Many chemical reactions, including this nitride reaction, are thermally activated. Increasing the temperature increases the kinetic rate constant as K_i of Equation 3. Thus, the rates of the homogeneous reactions for particle formation and heterogeneous reactions for thin film deposition increase with reaction temperatures. Sladek [16] proposed a quantitative model of homogeneous reaction in CVD processes for refractory compounds. His model showed that a homogeneous reaction was dominant as compared with a heterogeneous reaction at a temperature above a critical point. As the temperature increased beyond this critical point, the homogeneous reaction rate increased rapidly. The increase of powder formation rate with temperature shown in Fig. 4 can thus be explained. As temperature increases at constant r.f. current, homogeneous nucleation increases due to the enhancement of the reaction rate constant. Subsequently, increased numbers of nuclei grow into bigger particles through collision and coalescence along with deposition occurring on the particle surface. Temperature also played an important role in enhancement of crystallinity of particles, as shown in Fig. 5. Some reports [17, 18] on CVD processes mention similar temperature effects on crystallinity of coating or powder. In our process, the enhancement of crystallinity with temperature may be due to an increase of the desorption rate of the reaction products resulting from decomposition of TMAl in the plasma and absorbed on the particle surfaces, such as several types of hydrocarbon species produced in the plasma.

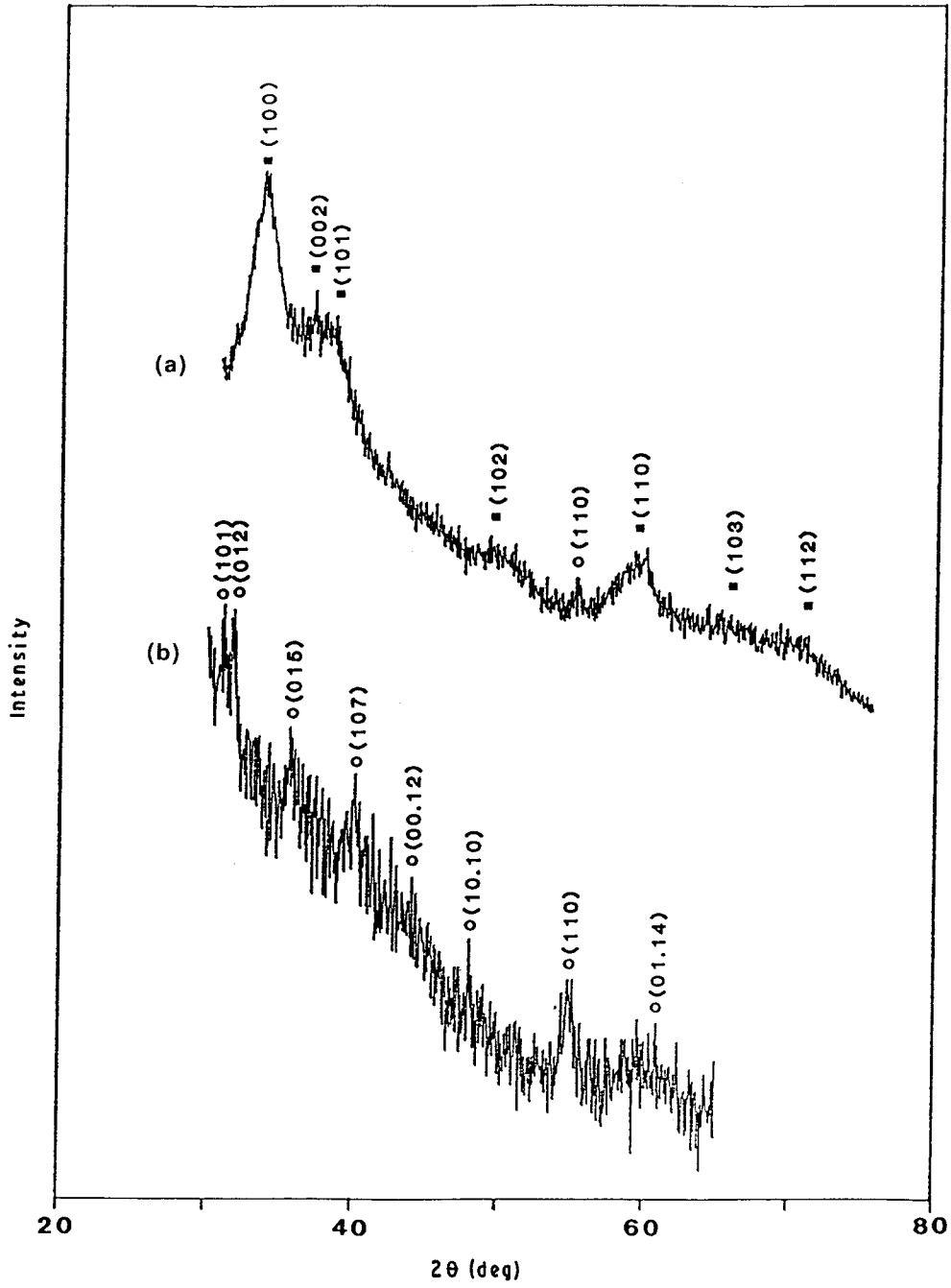

Figure 9 X-ray diffraction patterns showing the appearance of Al_4C_3 at high $TMAl/NH_3$ gas mixtures. (a) $TMAl/NH_3$ ratio 9×10^{-2}, NH_3 30 sccm; (b) TMAl was evaporated at the bubbler pressure of 10 torr, N_2 300 sccm (r.f. current 40 μA, susceptor temperature 770 °C, reactor pressure 10 torr). (■) AlN, (○) Al_4C_3.

4.3. Effect of reactant gas mixture

From Equation 3, the effect of TMAl concentration on particle formation rate seems to be evident. Increasing the TMAl concentration with relatively high amounts of inlet NH_3 gas increases the gas-phase reaction according to Equation 3. A high concentration of nuclei causes greater collision and coalescence together with deposition on the particle surfaces. Thus, the powder formation rate increases with TMAl concentration.

A high $TMAl/NH_3$ ratio produced by increasing the carrier nitrogen gas flow results in a mixture of AlN and Al_4C_3 as shown in Fig. 9a. Nitrogen gas is not regarded as a nitrogen source for the formation of AlN in our system, because the N≡N bond of nitrogen is stronger than the N–H bond of ammonia. Increase in the $TMAl/NH_3$ ratio results in a larger percentage of the Al_4C_3 phase in the powder. A powder consisting of single-phase Al_4C_3 is produced when only TMAl without NH_3 is used as shown in Fig. 9b. With insufficient nitrogen source for AlN formation, TMAl dissociates to form Al_4C_3 from the following stoichiometric relation [19]:

$$[Al(CH_3)_3]_4 \rightarrow Al_4C_3 + 9CH_4 \quad (4)$$

5. Conclusions

Ultrafine aluminium nitride particles were prepared in a cold-wall reactor by a plasma-assisted CVD method using the reaction between trimethylaluminium and ammonia. The effects of r.f. current, susceptor temperature and TMAl concentration on particle formation

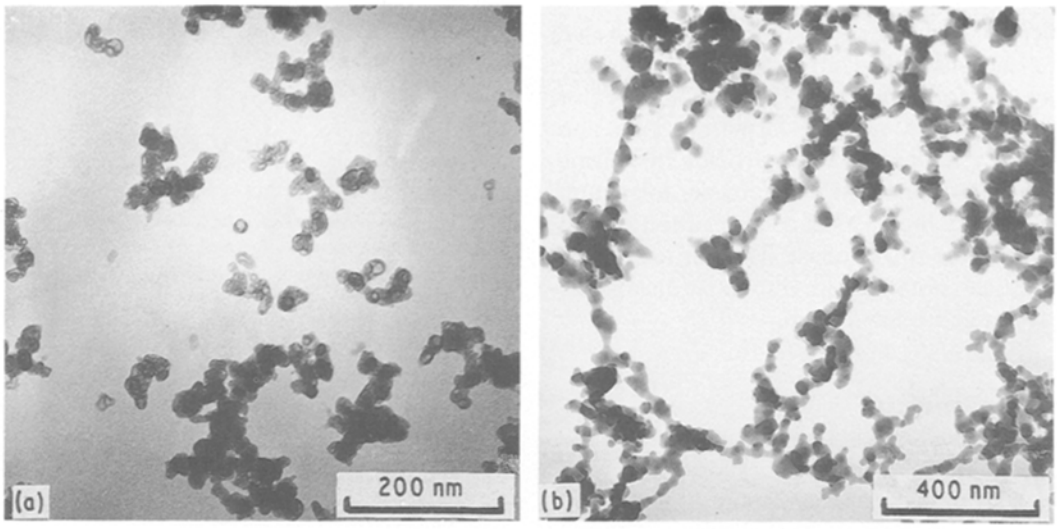

Figure 10 Transmission electron micrographs of particles prepared at the same condition as Fig. 9. (a) Photograph of particles of Fig. 9a; (b) Photograph of particles of Fig. 9b.

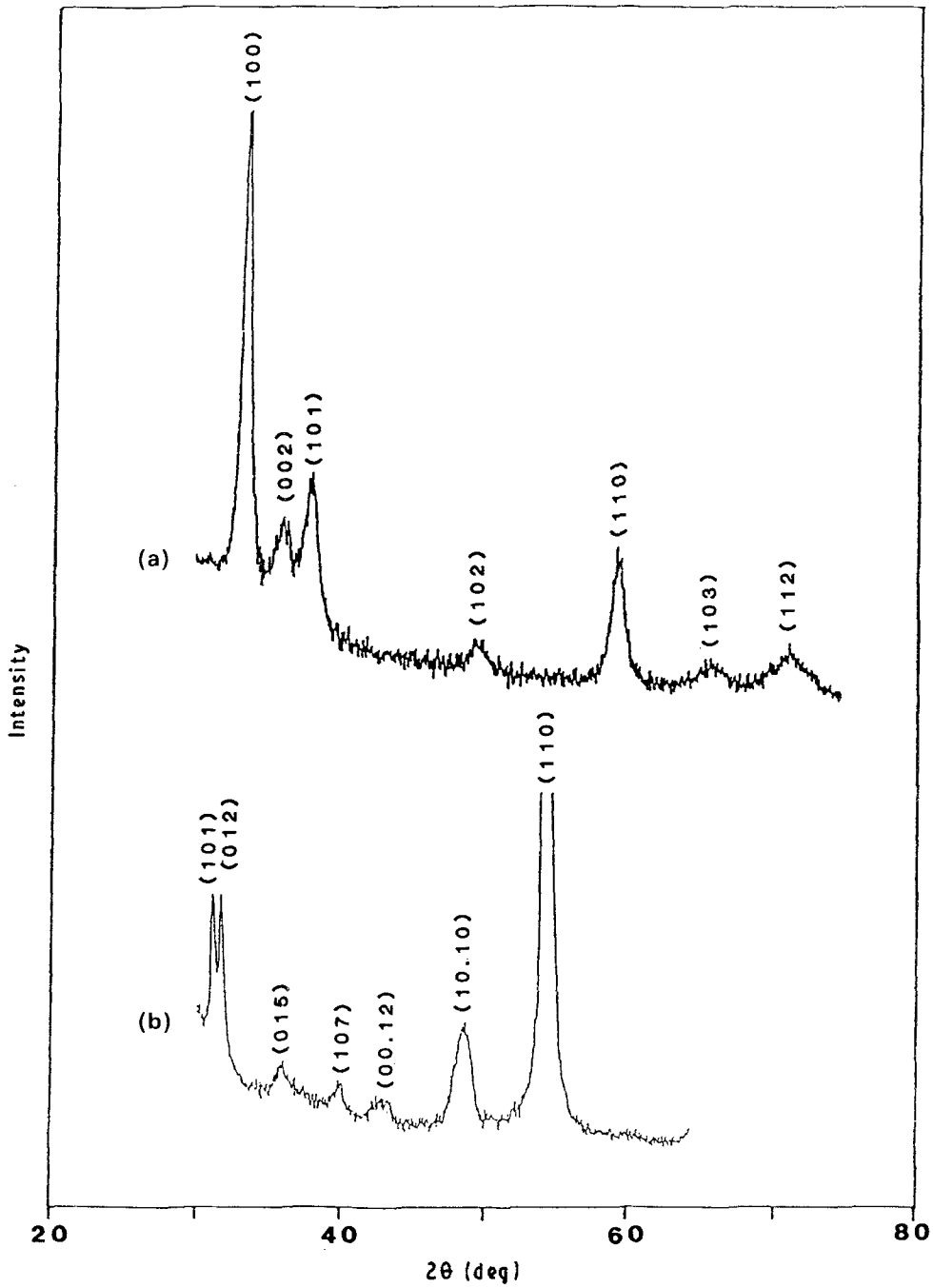

Figure 11 X-ray diffraction patterns of AlN film and Al_4C_3 film coated at the hot susceptor. (a) Diffraction pattern of AlN. (b) Diffraction pattern of Al_4C_3. (Deposition conditions are the same as in Figs 5c and 9b, respectively.)

were studied. A high r.f. current of 40 μA activated gas-phase reactions sufficiently to produce a considerable powder formation rate. Increase of susceptor temperature increased particle formation rate and enhanced the crystallinity of AlN particles. Increasing TMAl concentration increased the powder formation rate of AlN. A very high TMAl concentration caused the formation of the Al_4C_3 phase. The particle size of the AlN particle obtained in our experiment was estimated to range from 5–25 nm.

Acknowledgements

This work was funded under a research grant from the DIASYN Technologies Ltd. Support for K. H. Kim was obtained from Korea Science and Engineering Fellowship.

References

1. C. G. GRANQVIST and R. A. BUHRMAN, *J. Appl. Phys.* **47** (1976) 2200.
2. C. HAYASHI, *Physics Today* December (1987) 44.
3. D. FISTER, *Ceram. Engng Sci. Proc.* **6** (1985) 1305.
4. N. KURAMOTO, H. TANIGUCHI and I. ASO, in 36th "Electronic Components Conference" (IEEE, New York, 1986) pp. 424–9.
5. A. MATSUNAWA and S. KATAYAMA, *Trans. TWRI* **14** (1985) 190.
6. S. IWAMA, K. HAYAKAMWA and Y. ARIZUMI, *J. Crystal Growth* **66** (1984) 189.
7. S. PROCHAZKA and C. GRESKOVICH, *Amer. Ceram. Soc. Bull.* **57** (1978) 579.
8. S. IWAMA, K. HAYAKAWA and T. ARIZUMI, *J. Crystal Growth* **56** (1982) 265.
9. J. TOMIZAWA, O. TAKAI, S. TSUJIKAWA and S. GOTO, in "Proceedings of the International Engineers Congress – ISIAT '83 & IPAT '83", edited by T. Takagi (Institute of Electrical Engineers of Japan, Tokyo, 1983) pp. 1411–16.
10. W. KERNER and V. S. BAN, in "Thin Film Processes", edited by J. L. Vossen and W. Kern (Academic Press, New York, 1978) p. 257.
11. J. J. WU, H. V. NGUYEN and R. C. FLAGAN, *Langmuir* **3** (1987) 266.
12. "Powder Diffraction File", Joint Committee on Powder Diffraction Standards (American Society for Testing and Materials, Philadelphia, 1976).
13. J. FEDER, K. C. RUSSELL, J. LOTHE and G. M. POUND, *Adv. Phys.* **15** (1966) 111.
14. H. M. MANASEVIT, F. M. ERDMANN and W. I. SIMPSON, *J. Electrochem. Soc.* **118** (1971) 1864.
15. A. T. BELL, in "Techniques and Applications of Plasma Chemistry", edited by J. R. Hollahan and A. T. Bell (Wiley Interscience, New York, 1974) p. 31.
16. K. J. SLADEK, *J. Electrochem. Soc.* **118** (1971) 654.
17. S. B. KIM, S. C. CHOI, S. S. CHUN and K. H. KIM, *J. Vac. Sci. Technol.* **A9** (1991) 2174.
18. F. KIRKBIR and H. KOMIYAMA, *Mater. Res. Soc. Symp. Proc.* **121** (1988) 268.
19. L. M. YEDDANAPALLI and C. C. SCHUBERT, *J. Chem. Phys.* **14** (1946) 1.

Received 29 January
and accepted 7 June 1991